AUTOMATIC NDT ANALYSIS OF X-RAYED WELDING IMAGES

Andrea Bracciali, Monica Carfagni, and Paolo Citti
Dipartimento di Meccanica e Tecnologie Industriali
Universita' di Firenze, Firenze, Italy

ABSTRACT

Digital image processing is commonly used in nondestructive testing (NDT) to improve the quality - i.e., legibility - of x-rayed images. In the case of weld radiography, however, the subsequent critical steps of image analysis and defect location-classification are normally carried out by human operators, who are inevitably prone to subjective diagnosis errors.

This work presents software designed by the authors to automatically analyze x-rayed weldings, which may be adapted to any database. In experimental testing, the algorithms developed were successful in automatically locating and classifying defects on radiographic images.

INTRODUCTION

Welding is one of the processes most commonly used to connect metal components. However, whenever high safety levels are imperative, nondestructive testing (NDT) - albeit costly - must be performed to ensure the reliability of the welded connection. Using NDT techniques, normally x-rays, gamma rays, or ultrasounds, we can pinpoint defects in the welding area such as inclusions, porosities, blowholes, lack of penetration of the weld material, sticking, cracks, and cuts. Acceptability can then be determined on the basis of the size, type, and location of the defect(s).

Acceptability criteria are normally indicated in tables. These tables, which establish the worst conditions of each defect's characteristic geometric parameters that are acceptable for joint functionality, also account for the influence of the relative position of the defect(s). The fact that each defect is rated in context and never - except for unacceptable defects - on a strictly individual basis is important in view of the possibility that, under stress, groups of theoretically negligible microdefects can generate a single, far more serious defect.

The main problem in x-ray examination, despite recent advances in radiometallurgical techniques, is the lack of automated processes for fundamental steps such as defect location and classification from radiographic images. The result is that test reliability varies in relation to human factors such as the operator's level of attention and skill. The tasks of evaluating x-ray images are carried out by human beings who are inevitably prone to limited attention spans, and whose judgment is necessarily based upon a restricted body of knowledge.

To automate this process, we designed the software for an automatic diagnostic station for x-rayed welds. It is characterized by open architecture and is adaptable to specific requirements - a notable advantage when the acceptability criteria must be modified and/or when the database must be expanded. The solutions were developed and verified on an experimental station built around a PC with a graphics card to digitize and process the image. A camcorder was used to enable image acquisition from x-ray plates. Despite inevitable hardware limitations, primarily in terms of processing speed, the setup proved capable of performing the tasks for which it was developed.

THE STRUCTURE OF THE ALGORITHMS

The complete processing procedure entails the following logical flow steps:

Step 1. Acquiring and digitizing the x-ray image.
Step 2. Transforming the image. This step comprises:
- reducing "noise" through prefiltering
- determining the welding seam contours
- filtering out the welding seam background
- binarizing.

Step 3. Interpreting defects. This step comprises:
- extracting defect boundaries
- extracting defect typical geometries

Step 4. Classifying defects and issuing reports.

While steps 3 and 4 resemble the operations normally carried out by an operator, steps 1 and 2 are typical of an automatic image processing and recognition system such as the diagnostic station we have developed.

During digitization, the image acquired by the camcorder is divided into discrete points and transformed into a set of numbers (matrix). Each number in the matrix is associated to an area on the screen and assigned a value representing the point's gray level. Using eight bits per point, zero is associated to black and the highest number, 255, to white. It is helpful to consider the matrix as a function f(i,j) that associates a gray level to each image point in column i and row j, which we have termed "gray function." In radiographic applications, the chromatic content is low enough to allow use of a simplified monochromatic digitalization.

THE TRANSFORMATION OF THE IMAGE

The digitized radiographic image of the weld, while legible by a human operator, is illegible to an automated system, which requires accurate image processing. As opposed to the human eye, which is even able to pick defects out of a notably heterogeneous background, automated systems can only find defects which clearly stand out from the background. Hence, it is necessary to process the image in successive filtering steps until binarization is attained - that is, until the image is reduced to only two levels of gray. The defect can then be associated to one of the grays, the background to the other.

A radiographic image obtained on the experimental station monitor is shown after digitization in Figure 1 and after final processing in Figure 2. The dark spots in Figure 2 are the defects visible in Figure 1, which now stand out on a perfectly homogeneous ground. Assuming that the weld develops linearly - which, for that matter, is not overly restrictive - we can process the image by working on parallel sections normal to the seam's geometric axis.

We can now consider the radiographic image as the sum of three superimposed images, and thus the gray function as the sum of the following functions:
- fs(i,j), the function associated with the ideal weld seam,
- fd(i,j), the function associated with defects and representing the unknown to determine, and
- fn(i,j), the function associated with the "noise," i.e., the disturbances from slight random variations arising during x-raying, that is to say:

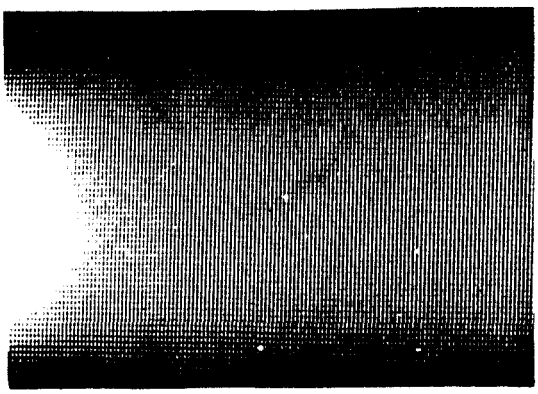

Fig. 1 Unprocessed x-rayed image.

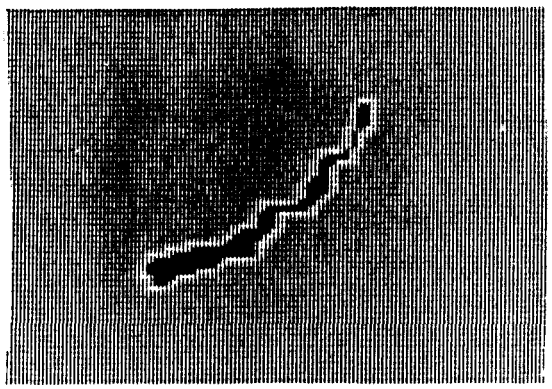

Fig. 2 Processed x-rayed image.

$$f(i,j) = fs(i,j) + fd(i,j) + fn(i,j)$$

Figure 3 shows the f(i,j) function for an image column, i.e., a section of the seam with constant i values. Note the cavity caused by the defect.

1. Prefiltering

Prefiltering, the first step in transforming the image and thus in determining fd(i,j), consists of smoothing out the gray function for the purpose of reducing noise in the image columns and thus on the total image. It is carried out section by section along the image column. Each new value at the point of the j ordinate is calculated as the mean of the values in the same ordinate and in the two neighboring ones. The result is comparable to those obtainable with a low-pass filter.

Although smoothing can be carried out more than once, it should be used with moderation. While it notably reduces noise, it could also cause a decrease in contrast, which would mean a loss of the defect's geometric details. The column illustrated in Figure 3 is shown after prefiltering in Figure 4.

2. Determining the Welding Seam Contours

The determination of the welding seam contours is extremely important. The difference in the degree of peril between two identical defects lies in their localization inside the welding seam. The system's knowledge of the seam contours creates the reference used in evaluating defect location.

This step must necessarily be carried out prior to filtering, after which it would be worthless, and after prefiltering, because this routine can be affected by the noise. Like prefiltering and filtering, it is based on a section-by-section processing of the graphic window.

Determination of the welding seam contours requires thresholding. The threshold below which the algorithm attributes the point to the welded component and above which to the welding seam is determined as the linear function of the means between the minimum and maximum grays of each image column. The coordinates of the points are then saved on a vector to be used in the successive processing stage.

3. Filtering

The operator can recognize defects inside the welding seam because their gray level differs from the background's: The majority of defects are darker gray, while material inclusions and oxides are lighter gray on account of their greater radio-opacity. The automatic system must use the same photometric properties to locate the defect. Unfortunately, since the background is not homogeneous, we would not obtain sufficiently reliable results by applying the procedure directly to the radiographic image. The welding seam shape and the weld's surface irregularities create a background with exceedingly variable gray tones. Under such circumstances, it is impossible to directly use the threshold procedure, since a different threshold would be needed at each point of the welding seam to ensure that the defect is distinguishable from the background.

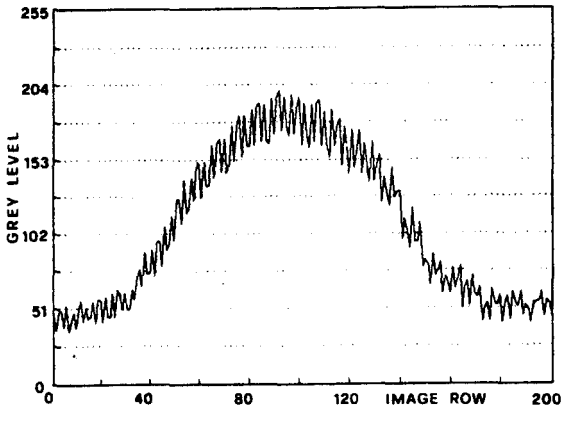

Fig. 3 Gray function f(i,j).

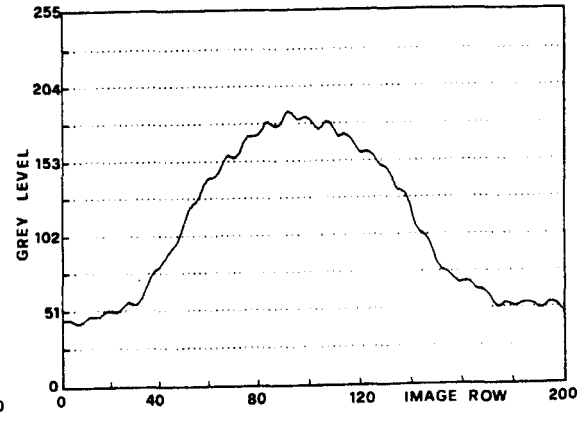

Fig. 4 Gray function $f_g(i,j)+f_d(i,j)$.

As previously mentioned, the radiographic image can be viewed as the superimposition of three separate images. Assuming that the noise has been eliminated in prefiltering, we can proceed to filtering to rid the image of the background which describes the welding seam shape, thereby obtaining a homogeneous background from which only the defects stand out. Care must be taken not to alter the defects' geometries so recognition is not affected. If this operation is successful, we obtain fd(i,j). The result will be approximate in terms of residual noise and imperfect correspondence of fs(i,j) to the actual welding seam contour.

Our first step was to calculate the background function fs(i,j) by a special interpolation procedure with a family of B-spline curves. (The mathematical procedure is described in Giloi, 1987.) The B-splines are relatively easy to use and lack the "waviness" typical of polynomial curves. In addition, the B-spline curves are only slightly affected by variations in one of the points upon which the passage is imposed, except for the zone around the point itself.

To ensure the reliability of the method, it should be observed that if one of the n+1 points of the interpolation belongs to a defect region, the curve will not accurately represent the background function, but rather one of its combinations with the gray function associated to the defects. This would give rise to an incorrect result after filtering. To prevent this, two spline curves with sets of defining points offset by a length δ are calculated. It is assumed that if one of the curve's interpolation points turns up inside the defect zone, the corresponding point on the other spline will not. This derives from the assumptions that the transversal development of defects exceeding δ have already been eliminated and that clear defects have already been determined by a simple threshold procedure. Point by point, the higher value of the two splines is accepted as fs(i,j), since the clear defects are assumed as already classified.

This procedure requires the selection of the optimal values for δ and n+1, but the tests carried out have shown a low sensitivity of the method to these values. At this point, we can subtract fs(i,j) from prefiltered f(i,j).

Splines calculated for the filtering of two sections are shown in Figures 5 (without defect) and 6 (with defect). The splines are superimposed on the gray function curve after prefiltering of the sections.

4. Binarization

One threshold is not enough to pick out the defect, since the resulting image can be affected by disturbances. While, on the one hand, a very high threshold value would enable excellent discrimination between defect and disturbances (which never reach the same gray tones), but would significantly alter defect geometries, on the other, a very low value would not affect defect geometries, but would fail to eliminate any disturbances.

For this reason, two thresholds are used. The first, extremely severe, is used to pick the defect out of the surrounding disturbances. The points attributed to the defect zone are then stored and used in the second threshold. The second threshold

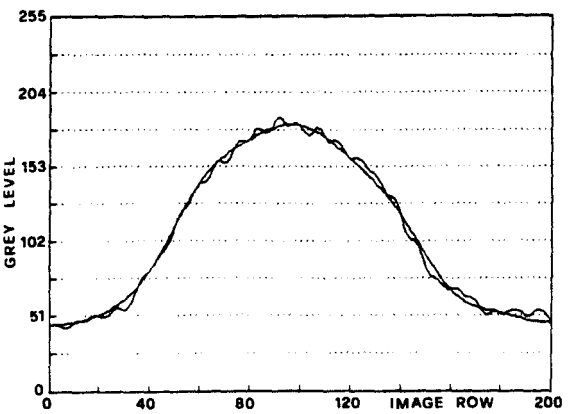

Fig. 5 B-spline curve superimposed on a gray function curve (without defect).

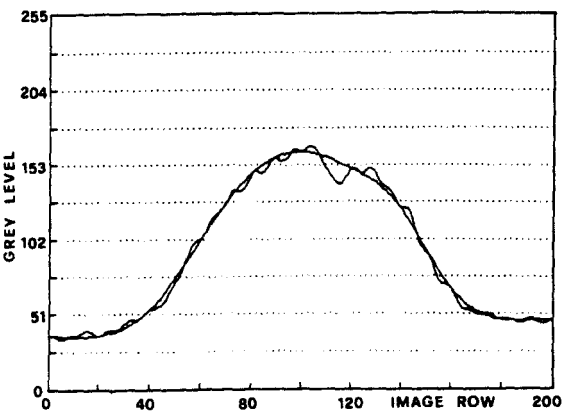

Fig. 6 B-spline curve superimposed on a gray function curve (with defect).

can be applied solely in the vicinity of these points, since, being much lower than the first, it does not alter the defect's geometry. Thanks to this procedure, we can combine the advantages of high and low level thresholds, while reducing the criticality of the single threshold level.

The processed image is shown in Figure 2. It is termed "binarized," since it is composed of only two gray tones: black for defects, medium gray for all other points.

Our last step is to eliminate the black pixels that are isolated from the defect zone. Two routines directly available from the graphic board management library perform this task: The first, Erode, coalesces the isolated dark pixels that are never far from the other dark areas, while the second, Dilate, eliminates the isolated pixels.

At this point, the image transformation is complete and the defects are perfectly revealed, ready for the next routine.

CLASSIFYING THE DEFECTS AND ISSUING A REPORT

After processing, the image must be interpreted so that the defects may be characterized. The first step is to extract the contour of the defect and then analyze its geometric characteristics. The information needed in classification includes localization of the defect, its area, its thickness, and the axis of the defect's greatest development.

1. Determining the Defect's Geometric Characteristics

A scanner - actually a "cursor" the size of a pixel which autonomously moves over the image field - was used to extract the contour. First, it scans the image looking for a black point, i.e., a point that belongs to the defect. When one has been found, it begins to rotate leftward one pixel. If the next point belongs to the defect, it rotates another pixel leftward, otherwise, it rotates one pixel rightward. In this way, the cursor touches all the contour points, rotating round the defect clockwise until returning to the starting point. All the scanned contour points are then stored in a vector, and the gray tones of contour pixels are whitened to simplify the successive algorithms for the extraction of the geometric properties (Figure 2).

The localization of the defect can be associated to the coordinates of the centroids of the contour points. To evaluate the defect area, we count the pixels inside the contour (recalling that a pixel does not necessarily cover a square area). The defect's major axis is considered the axis that intersects the pair of contour points farthest apart with respect to any other pair of points. Once this pair has been found, it is simple to calculate the angular coefficient of the straight line joining them.

Having determined this axis, we can calculate the size of the defect in the direction normal to that of the major axis, which is essential in characterizing the defect. The calculation comprises two steps: The contour points are divided into two groups by the major axis; for each group, the distances between the points and the major axis are evaluated. Then, the maximum distances found for each group are summed together in order to determine defect size in the direction normal to the major axis.

At the end of the extraction step, an algorithm must be developed to calculate the behavior of the defect thicknesses. Since the concept of the thickness of a geometric figure is not as clear-cut as would appear, it was necessary to establish an exact definition of thickness: We define thickness of the figure at contour point Pi as the length of the segment which joins Pi to a second point. The second point must have this property so that the angles that the segment forms with the straight lines tangent to the contour in point Pi and the second point are equal.

In keeping with this definition, we developed the algorithm for determining thickness. For each contour point, the straight line normal to the contour is determined, after which the other point that the line intersects on the contour is calculated. We then evaluate the angles that this normal line forms with the tangents at the contour points intersecting the line. If the angles are equal, the thickness is calculated as the distance between the two points. Otherwise, we proceed iteratively until it is possible to determine the inclination other than 90° to be assigned to the line intersecting the contour. Having determined the line, we can then calculate thickness as the distance between the two points where the line intersects the contour.

2. Recognizing and Classifying a Defect

An algorithm was also developed to assign a type to each defect and to compile a report for the NDT operator. An essential contribution to our work was the experience and knowledge acquired by actual NDT operators dealing with NDT radiometallographic welding problems on a daily basis. Since, however, each company uses different quality standards, we felt it would be important to develop an algorithm adaptable to specific requirements.

The defect recognition algorithm is a tree algorithm in which the system compares its knowledge of the defect against a series of alternative logics until it arrives at a terminal branch corresponding to a precise defect typology. Having established the nature of the defect, we can use a second control logic tree to verify whether the defects, either individually or in relation to the welding seam or its reciprocal, fulfill the qualitative standards imposed by user-selected standards. The excellent results also derived from the constancy of the boundary conditions and the excellent contrasts in the radiographic images. Our next step will be to further enhance the programs by implementing autosetting functions.

RESULTS

The algorithms were converted into an executable program and then implemented on the experimental diagnostic station. Preliminary verification and honing of the algorithms was obtained by applying them to a vast "simulated" sampling and then testing by using them to process actual radiographic segments. The testing, which was carried out on radiographs with defects differing as to type and location in relation to the welding seams, fully validated the algorithm. No defects "vanished" during filtering, and each one was correctly recognized according to the set standards.

CONCLUSIONS

This work presents algorithms developed to manage an automated welding diagnostic system based on the digital analysis of radiographic images. The system provides the NDT operator with a report on defects in the welding seams, their size, location, direction, and nature. Three steps are required: 1) processing the image to increase legibility, 2) filtering the image to pick the defect out of the rest of the image components, and 3) extracting the geometric characteristics needed to classify the defect. The decisional logic structure used in the defect recognition-classification phase is based upon data obtained from user-selected standards. The proposed system was amply validated on an experimental test station.

ACKNOWLEDGMENTS

This work was supported by the Consiglio Nazionale delle Ricerche (Italy).

REFERENCES

Cappellini, V., 1985, Elaborazione numerica delle immagini, Boringhieri, Turin, Italy.

Carfagni, M. and Citti, P., 1988, "Automatic Image Processing and Recognition for Diagnosing Mechanical Systems," *Proceedings, International Condition Monitoring Conference*, Atlanta, Georgia.

Daum, W., Rose, P., Heidt, H., and Builtjes, J.H., 1971, "Automatic Recognition of Weld Defects in X-Ray Inspection," British Journal of NDT.

Duda, R.O. and Hart, P.E., 1973, Pattern Classification and Scene Analysis, John Wiley, New York, New York.

Gilardoni, A., Orsini, A., and Taccani, M., 1981, NDT Handbook, Mandello Lario, Como, Italy.

Giloi, W.K., 1987, Interactive Computer Graphics, Prentice-Hall, Englewood, N.J.

Janney, D.H., 1979, "Image Processing in Non-Destructive Testing," *Proceedings, 23rd Sagamore Army Material Research Conference*, Plenum Press, New York, New York.

Koshimizu, H. and Yoshida, T., 1983, "A Method for Visual Inspection of Welding by Means of Image Processing of the X-Ray Photograph," *Transactions of the IECE of Japan.*